Longitudinal Impedance Measurements on Graphene QHE Devices

(Article begins on next page)

Longitudinal Impedance Measurements on Graphene QHE Devices

Frédéric Overney[1], Ali L. Eichenberger[1], Stephan Bauer[2],
Massimo Ortolano[3], Martina Marzano[4], Yefei Yin[2] and Mattias Kruskopf[2]

[1]Federal Institute of Metrology METAS, Bern, Switzerland
[2]Physikalisch-Technische Bundesanstalt, Braunschweig, Germany
[3]Politecnico di Torino POLITO, Torino, Italy
[4]Istituto Nazionale di Ricerca Metrologica INRIM, Torino, Italy
E-mail: frederic.overney@metas.ch

***Abstract*—This paper addresses the challenges associated with accurately measuring longitudinal impedance in a quantum Hall device. A novel bridge design capable of measuring both real and imaginary components of longitudinal impedance is introduced and applied for the first time. The measured inductance appears to be independent of both carrier density and mobility. Additionally, the inductance remains constant over the frequency range from 600 Hz to 50 kHz.**

***Index Terms*—Quantum Hall Effect, graphene, precision measurements.**

I. Introduction

Since the redefinition of the SI [1], fixed values have been assigned to the elementary charge (e) and the Planck constant (h). Consequently, the quantum Hall effect (QHE) has become a practical realization of the ohm, the unit of electrical resistance [2]. However, it is crucial to adhere to the guidelines established by the CCEM [3] when employing the quantum Hall effect. These guidelines encompass several recommendations, including stipulating that the quantum Hall resistance should be measured under dissipation-less conditions, specifically using a two-dimensional electron gas (2DEG) where the longitudinal resistance approaches zero.

While measuring the longitudinal resistance in DC is relatively straightforward, the scenario becomes considerably more intricate when dealing with AC. The stray admittance of the coaxial cables employed to connect the QHE device (maintained at low temperature) to the measuring instrument (at room temperature) presents a challenge. This stray admittance loads the 2DEG, making it difficult to accurately measure the longitudinal voltage drop, denoted as V_{xx}, along the side of the QHE device.

After the first AC QHE measurement [4], dedicated bridges were developed and optimized for accurate measurement of the AC dissipation on both sides of the QHE device at frequencies up to a few kHz [5], [6]. However, the balancing procedure of existing bridges is mostly manual and requires skilled operators.

More recently, a new fully automated bridge has been proposed [7] to measure both the real and the imaginary part of the longitudinal impedance Z_{xx}. The first results obtained using this bridge are reported for a single graphene device (G1511-41-96) fabricated at PTB.

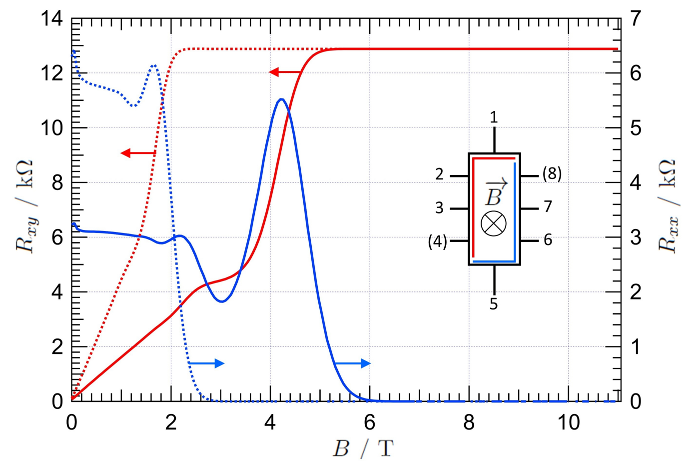

Fig. 1. Magnetoresistance measurements performed at 4.2 K during two measurement campaigns. The sample was left at room temperature and in ambient air between the two campaigns. Solid lines: first campaign. Dashed lines: second campaign.

II. Device characteristics.

The Hall bar is fabricated from epitaxial graphene and is depicted in the inset of Fig. 1. The Hall bar has a total length of 1600 µm, a width of 400 µm, and features eight electrical contacts labeled from 1 to 8. The distance between two neighboring lateral contacts is 400 µm.

The Hall bar is mounted on a TO-8 sample holder. Only six of the eight contacts on the Hall bar are connected with aluminum (Al) wires to the pins of the chip carrier. Contacts 4 and 8 remain unconnected. For the current contacts (labeled 1 and 5), two Al wires are bonded in parallel, while a single Al wire is used for the potential contacts (labeled 2, 3, 6, and 7).

Figure 1 illustrates the characterization of the DC properties of the device measured at 4.2 K across two distinct measurement campaigns. The sample was exposed to ambient air at room temperature for a duration of 14 days between the two campaigns.

During this interval, the carrier density of type n decreased from $3.88 \times 10^{11}\,\mathrm{cm}^{-2}$ to $1.47 \times 10^{11}\,\mathrm{cm}^{-2}$, while the mobility increased from $5.15 \times 10^{3}\,\mathrm{cm}^2/(\mathrm{Vs})$ to $7.14 \times 10^{3}\,\mathrm{cm}^2/(\mathrm{Vs})$.

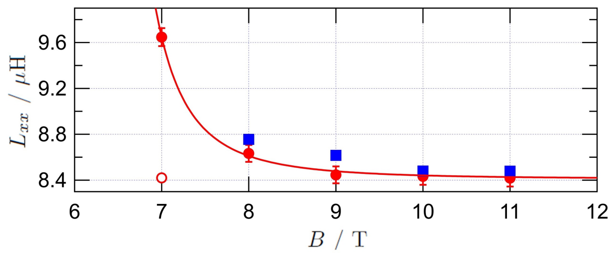

Fig. 2. Magnetic field dependence of the longitudinal inductance measured at a temperature of 4.2 K and a frequency of about 5 kHz. Solid symbols represent values obtained during the first campaign using the METAS bridge (red circles) and the INRIM-POLITO bridge (blue squares), while the open symbol represents a value obtained during the second campaign using the METAS bridge. The solid line is just a guide for the eyes.

III. Preliminary Results

Figure 2 depicts the longitudinal inductance L_{xx} measured on the low side (between contacts 7 and 6) using both the METAS bridge (red circles) and the INRIM-POLITO bridge (blue squares) at a frequency of approximately 5 kHz. The initial value of about 9.6 µH at 7 T diminishes gradually with increasing magnetic field density. Beyond 9 T, the value stabilizes at approximately 8.41 µH. This behavior is consistent with the measurements obtained using the INRIM-POLITO bridge. The INRIM-POLITO bridge has been implemented according to the principle of the METAS bridge [7] by modifying the network of the fully-digital bridge described in [8].

During the second campaign, a measurement was conducted at 7 T (open circle). As anticipated from the magnetoresistance measurements (see Fig. 1), the quantization occurs at a lower magnetic field, and the inductance value achieved at higher magnetic fields in the first campaign is already reached at 7 T. Although further measurements are required to confirm this assertion, it appears that the measured L_{xx} in the quantized state is independent of both the carrier density and the mobility.

In the second campaign, the frequency dependence of the longitudinal impedance $Z_{xx} = R_{xx} + \mathrm{j}\omega L_{xx}$ was measured at 7 T from 600 Hz to 50 kHz. The results are presented in Fig. 3. L_{xx} demonstrates clear independence from frequency, whereas R_{xx} exhibits a linear increase with frequency up to 30 kHz. Above this frequency, the slope seems to steepen.

Two different interpretations of the measured longitudinal inductance L_{xx} exist. A similar value of inductance has been observed in GaAs samples within the same frequency range, where the observed inductance is associated with the effective quantum inertia of the charge carriers [9]. Alternatively, the inductance may be attributed to magnetocapacitance and dissipation factor within the 2DEG [10].

Comprehensive DC and AC characterizations of various devices conducted in different laboratories will be presented at the upcoming conference.

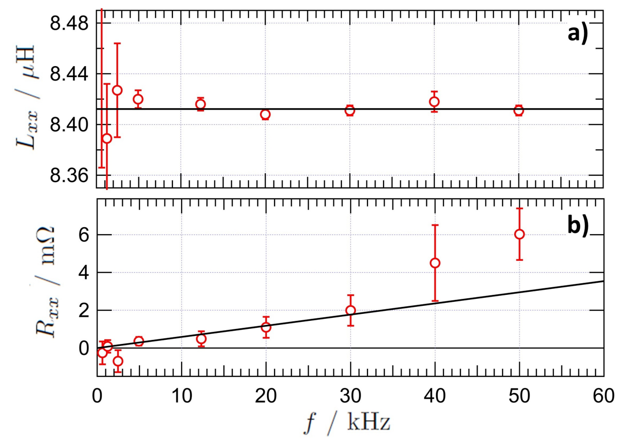

Fig. 3. Frequency dependence of both L_{xx} (a) and R_{xx} (b) measured during the second campaign at a temperature of 4.2 K and a magnetic field density of 7 T. The solid lines represent constant inductance L_{xx} of 8.412 µH and a resistance R_{xx} proportional to frequency with a coefficient of 59 µΩ/kHz. The uncertainty bars correspond to Type A uncertainty (k=1).

IV. Conclusion

A novel bridge design has been implemented by METAS and INRIM-POLITO, allowing for the investigation of both the real and imaginary parts of the longitudinal impedance (Z_{xx}) of a quantum Hall effect (QHE) device. The longitudinal inductance has been measured on a graphene sample. Both bridges yield a value of approximately 8.4 µH at magnetic field densities above 9 T. This new bridge represents a promising tool for investigating the AC transport properties of a 2DEG.

References

[1] M. Stock, R. Davis, E. de Mirandés, and M. J. T. Milton, "The revision of the SI—the result of three decades of progress in metrology," *Metrologia*, vol. 56, no. 2, p. 022001, 4 2019.

[2] BIPM, "Mise en pratique for the definition of the ampere and other electric units in the SI," *SI Brochure-Appendix 2*, no. May, pp. 3–8, 2019.

[3] F. Delahaye and B. Jeckelmann, "Revised technical guidelines for reliable dc measurements of the quantized Hall resistance," *Metrologia*, vol. 40, no. 5, pp. 217–223, 10 2003.

[4] J. Melcher, P. Warnecke, and R. Hanke, "Comparison of precision AC and DC measurements with the quantized Hall resistance," *IEEE Transactions on Instrumentation and Measurement*, vol. 42, no. 2, pp. 292–294, 4 1993.

[5] F. Delahaye, "Accurate AC Measurements of the Quantized Hall Resistance from 1 Hz to 1.6 kHz," *Metrologia*, vol. 31, pp. 367–373, 1994.

[6] J. Schurr *et al.*, "AC longitudinal and contact resistance measurements of quantum Hall devices," *Metrologia*, vol. 43, no. 1, pp. 163–173, 2 2006.

[7] F. Overney, B. Jeanneret, and A. L. Eichenberger, "A New Bridge for Measuring the Longitudinal Impedance of a Quantum Hall Effect Device," in *2022 Conference on Precision Electromagnetic Measurements (CPEM)*. IEEE, dec 2022, pp. 1–2.

[8] M. Marzano, M. Ortolano, V. D'elia, A. Müller, and L. Callegaro, "A fully digital bridge towards the realization of the farad from the quantum Hall effect," *Metrologia*, vol. 58, no. 1, 2021.

[9] A. Delgard *et al.*, "Coulomb interactions and effective quantum inertia of charge carriers in a macroscopic conductor," *Physical Review B*, vol. 104, no. 12, p. L121301, 9 2021.

[10] M. Kruskopf *et al.*, "Graphene Quantum Hall Effect Devices for AC and DC Electrical Metrology," *IEEE Transactions on Electron Devices*, vol. 68, no. 7, pp. 3672–3677, 7 2021.